

Staining-Enhanced Peroxidase-Mimicking Gold Nanoparticles in Nano-ELISA for Highly Sensitive Detection of *Klebsiella pneumoniae*

Thu Thao Pham, Thien-Kim Le, Nguyen T. T. Huyen, Nam Luyen Van, Tin Phan Nguy, Dai Lam Tran, and Lien Truong T N*



Cite This: *ACS Omega* 2023, 8, 49211–49217



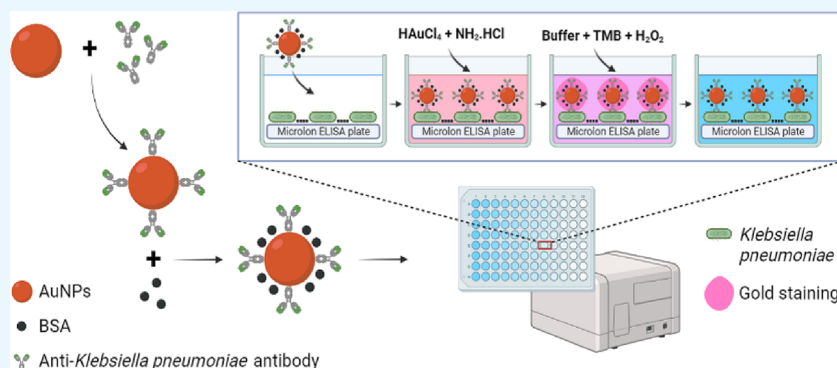
Read Online

ACCESS |

Metrics & More

Article Recommendations

Supporting Information



ABSTRACT: *Klebsiella pneumoniae*, a member of the family Enterobacteriaceae, is a rod-shaped, Gram-negative bacterium, mainly found in the hospital environment and medical tools. It is the leading cause of nosocomial infection, characterized by bloodstream infection, wound site infection, urinary tract infection, and sepsis, mostly in older adults, newborn infants, and immunocompromised patients. This present study demonstrated a novel diagnostic method for *K. pneumoniae* detection based on the gold nanozyme activity for the oxidation of 3,3',5,5'-tetramethylbenzidine (TMB) in the presence of H_2O_2 . The nanozyme activity of AuNPs with staining enhancement was statistically three times higher than that of the bare AuNPs in solid absorption at 650 nm. Nano-ELISA with staining enhancement could detect as low as 10^2 CFUs/mL of *K. pneumoniae* concentration, as the cutoff value was determined to be 0.158, which boosted the sensitivity of the immunoreactions by up to 100-fold. The detection limit of our assays was 26.023 CFUs/mL, and the limit of quantification was 78.857 CFUs/mL. There was no cross-reaction against other bacteria, which proved the immunoassays' remarkable specificity for recognizing *K. pneumoniae*. Taken together, we successfully developed and optimized the highly sensitive and decently specific nano-ELISA strategy that might be applicable for detecting various other bacterial pathogens.

1. INTRODUCTION

Klebsiella pneumoniae is a significant Enterobacteriaceae considered one of the opportunistic pathogens causing broad spectra of severe diseases and clinically crucial organisms that have acquired much public health concern.¹ It parasitizes the respiratory or intestinal tracts of humans and animals. It probably causes zoonotic diseases such as meningitis, pneumonia, urinary tract inflammation, and even sepsis in the clinical veterinarian, contributing to enormous potential threats to human health and livestock production.² In Western countries, up to 5% of healthy humans in the community are nasopharyngeally colonized by *K. pneumoniae*, and this proportion may be as high as 30% in Asian countries. In healthy individuals in Western countries, the colonization of the gastrointestinal tract ranges from 5 to 35%, which can reach up to 60 to 70% in Asian countries.³ Therefore, developing susceptible and specific methods for *K. pneumoniae*

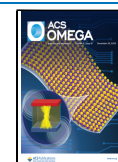
detection is urgent. Conventional methods are regarded as the gold standards for *K. pneumoniae* detection, including pure culture, microscopic determination, and biochemical examination. However, these phenotype-based techniques were labor-intensive, time-consuming, and easily contaminated by other bacteria.⁴ Other genotype-based methods, such as polymerase chain reaction (PCR) or sequencing, are rapid, accurate, and widely applied in clinical and microbiological laboratories.⁵ Nevertheless, these methods could not be performed in low-

Received: September 28, 2023

Revised: November 20, 2023

Accepted: November 27, 2023

Published: December 13, 2023



resource-setting areas that lack precise equipment and trained personnel.

The application of enzyme-mimicking nanoparticles (nanozymes) has gained popularity as it overcomes the drawbacks of natural enzymes (i.e., less stability in harsh environmental conditions, cost-effectiveness, and storage difficulty) in the case of colorimetric biosensor development for point-of-care (POC) diagnosis.⁶ The peroxidase mimic catalytic activity of nanoparticles could catalyze H₂O₂ to oxidize the substrates such as 3,3',5,5'-tetramethylbenzidine (TMB) or 2,2'-azinobis(3-thylbenzothiazoline)-6-sulfonic acid (ABTS) to develop blue-green or turquoise colors, respectively. In recent years, the nanozyme activity of AuNPs has been developed as an ultrasensitive colorimetric pH indicator for urea, urease, and urease inhibitor detection,⁷ *Mycobacterium bovis* detection using biogenic AuNPs produced from fruit extract,⁸ dopamine, and glucose,⁹ and *Staphylococcus aureus* detection.¹⁰

In line with this, we develop and evaluate the nanozyme activity by participating in an ELISA assay for *K. pneumoniae* detection. As far as we know, our report describes the first nano-ELISA techniques utilizing the AuNPs–antibody conjugation to detect *K. pneumoniae*. This biosensing technique based on the nanozyme activities could be widely used to develop quick, cost-effective, on-site detection of pathogens, biomarkers, or toxins indicating human or animal diseases or contamination in food and water.

2. MATERIALS AND METHODS

2.1. Materials. Gold(III) chloride solution (HAuCl₄, 99.99% trace metals basis), bovine serum albumin (BSA, ≥98%), 3,3',5,5'-tetramethylbenzidine (TMB substrate, ≥99%), acetic acid (glacial, ≥99.7%), Tween-20 (≥40.0%), brain heart infusion broth (BHI broth), and agar were purchased from Sigma-Aldrich Co., Ltd., USA. Trisodium citrate dihydrate (HOC(COONa)(CH₂COONa)₂·2H₂O, ≥99%), hydroxylammonium chloride (NH₂OH·HCl, ≥99%), hydrogen peroxide (H₂O₂, 30%), sodium acetate trihydrate (CH₃COONa·3H₂O, ≥99%), sodium chloride (NaCl, ≥99%), potassium chloride (KCl, ≥99%), disodium hydrogen phosphate (Na₂HPO₄, ≥99%), and potassium dihydrogen phosphate (KH₂PO₄, ≥99.5%) were purchased from Merck, USA. *K. pneumoniae* polyclonal antibody (Rabbit, IgG) was purchased from Invitrogen, USA. Immunoreactions were performed in Pierce 8-Well Polystyrene Strip Plates, Corner Notch (Thermo Scientific, Inc., USA).

2.2. Bacteria Strains. *K. pneumoniae* (VTCC 12273) and *Pseudomonas aeruginosa* (VTCC 12018) were provided by the Institute of Microbiology and Biotechnology, Vietnam National University. *Escherichia coli* (ATCC 25922), *Clostridium perfringens* (ATCC 12915), *S. aureus* (ATCC 11632), and *Salmonella typhimurium* (ATCC 14028) were purchased from Kwik-Stik, Microbiologics Inc., USA. The strains were grown at 37 °C in BHI broth until an optical density (OD) at 600 nm of 0.8 (10⁸ CFU/mL) was reached. *P. aeruginosa*, *E. coli*, *C. perfringens*, *S. aureus*, and *S. typhimurium* were used as negative controls. *K. pneumoniae* and the negative controls were cultured in BHI agar to determine the serial dilution and calculate CFUs/mL. The bacteria were cryopreserved in glycerol and stored at −20 °C.

2.3. Synthesis and Characterization of Gold Nanoparticles. Gold nanoparticles were synthesized by Turkevich's method.¹¹ Briefly, 30 mM hydrogen tetrachloroaurate(III) hydrate was suspended in 150 mL of Milli-Q boiling water.

Then, dropwise, 34 mM trisodium citrate dihydrate was added to the boiling solution. The color changed gradually from light yellow to wine red. The synthesized gold nanoparticles (AuNPs) were cooled to room temperature and stored at 4 °C for further use. The AuNPs then were characterized by UV–vis spectroscopy (V-770 spectrophotometer, Jaco, Japan), dynamic light scattering and zeta potential (Zetasizer Nanoseries ZS Instrument, Anton Paar), and transmission electron microscopy (TEM) images operated at 200 kV (JEM-2011F microscope, JEOL, Japan).

2.4. Nanozyme Activity Optimization. The nanozyme activity was investigated by using TMB as a chromogenic substrate. We considered the concentration of the TMB substrate and H₂O₂ for optimizing the procedure. The assays were performed for TMB substrate concentration optimization in the polystyrene plate as follows: 25 μL of synthesized AuNPs was mixed with different amounts (0, 1, 2, 4, 8, 12, 16, 20, and 30 μL) of 10 mg/mL TMB solution and 15 μL of 30% H₂O₂. To optimize the concentration of H₂O₂, 25 μL synthesized AuNPs were mixed with 1.5 μL of 10 mg/mL TMB solution and different amounts of 30% H₂O₂ (0, 10, 20, 50, 75, 100, 150, and 200 μL). The reactions were measured at 650 nm by an absorbance microplate reader (Epoch, Biotek Instruments, Germany) every 2 min for 30 min.

2.5. AuNPs–Antibody Passive Conjugation. Physisorption optimization was done with 25 μL of synthesized bare AuNPs solution at pH 9.0. Different amounts (0, 1, 3, 5, 7, 10, 12, and 15 μL) of 100 μg/mL *K. pneumoniae* antibody (*Kleb* Ab) were added and incubated for 30 min. Then, the optimized amounts of the TMB substrate and H₂O₂ were added for the catalytic activity measurement. The reactions were measured at 650 nm every 2 min for 30 min.

For passive conjugation, 1 mL of AuNPs at pH 9.0 was incubated with an optimized amount of *Kleb* Ab for 30 min. After centrifugation for antibody excess removal, 1% BSA solution was added for blocking, and then the conjugated AuNPs–*Kleb* Ab was stored at 4 °C for further use.

2.6. Staining Enhancement Optimization. The staining procedure consists of two components including HAuCl₄ and NH₂OH·HCl concentrations. The optimized assays for HAuCl₄ concentration were carried out with 25 μL of synthesized AuNPs mixed with different concentrations (0, 1, 2, 5, 10, 15, and 20 mM) of HAuCl₄ and 80 mM NH₂OH·HCl. To optimize the concentration of NH₂OH·HCl, 25 μL of synthesized AuNPs was mixed with 1.5 mM HAuCl₄ and different concentrations (0, 10, 20, 30, 50, 80, 100, and 150 mM) of NH₂OH·HCl. The mixtures were incubated for 30 min. Then, the optimized amounts of the TMB substrate and H₂O₂ were added for the catalytic activity measurement. The reactions were measured at 650 nm.

2.7. Nano-ELISA and Staining Enhancement Procedures for *K. pneumoniae* Detection. A 100 μL portion of cultured *K. pneumoniae* in serial dilutions (10¹ to 10⁸ CFU/mL) was added into the wells and incubated overnight at room temperature. The next day, the wells were washed with PBS-T (1× PBS, pH 7.4, 0.05% Tween-20) and then blocked with 1% BSA for 1 h. After washing with PBS-T, 25 μL AuNPs–*Kleb* Ab conjugation was added to each well and incubated for 1 h at 37 °C. The wells were then washed and stained with HAuCl₄/NH₂OH·HCl. Fifty microliters each of optimized concentrations of HAuCl₄ and NH₂OH·HCl was added to each well. The wells were incubated for 30 min. The wells were washed three times, and then the TMB substrate and H₂O₂

were added to each well. Immunoassays were measured at the wavelength of 650 nm.

2.8. Specificity Determination. Nano-ELISA and staining enhancement were performed to detect *P. aeruginosa*, *E. coli*, *C. perfringens*, *S. aureus*, and *S. typhimurium* for the simultaneous specificity evaluation of the immunoassay simultaneously. The reactions were measured at 650 nm.

2.9. Cutoff Value, Limit of Detection (LoD), and Limit of Quantification (LoQ) Determination. The OD₆₅₀ values of 20 negative samples were measured by the nano-ELISA method. The mean and standard deviation of the OD₆₅₀ values were calculated. The cutoff value was measured by the mean value plus three times the standard deviation to determine whether a sample was positive or negative.

The LoD and LoQ were determined by the formulas:¹²

$$\text{LoD} = 3.3 \times \sigma/S$$

$$\text{LoQ} = 10 \times \sigma/S$$

σ and S are the slope of the standard curve and the standard deviation of blank samples, respectively.

2.10. Statistical Analysis. All the experiments were performed in triplicate, and differences between groups were analyzed using one-way ANOVA by GraphPad Prism (GraphPad Software Inc., La Jolla, CA, USA). Data for each group ($N = 3$) were expressed as the mean \pm standard error of the mean (SEM). Statistical significance was set at $p < 0.05$.

3. RESULTS AND DISCUSSION

3.1. Characterization of AuNPs. Gold nanoparticles have been widely employed in various fields based on their biocompatibility and multiple surface functionalities.¹³ One of the most well-known techniques for synthesizing AuNPs is based on reducing HAuCl₄ by citrate in water, which was used in this study.¹¹ The colloidal AuNPs were successfully synthesized in monodisperse suspensions by the standard citrate reduction method. The citrate reduction method could generate various sizes of gold nanoparticles depending on the molar ratio of trisodium citrate dihydrate to tetrachloroauric acid.¹⁴

Furthermore, the AuNPs displayed different levels of peroxidase-mimicking activity toward TMB in that the smaller the size, the higher the catalytic activity.¹⁵ Therefore, the spherical AuNPs' average size was synthesized as small as ~ 20 nm and $\sim 15 \pm 2$ nm, clearly validated by DLS analysis (Figure S1a) and TEM images (Figure 1a), respectively. The UV-vis absorbance spectrum of AuNPs had a characteristic peak at ~ 520 nm (Figure 1b), and the zeta potential was -21.85 mV (Figure S1b). It was reported that negatively charged materials were in favor of the oxidation of the cationic substrate TMB.¹⁶ Therefore, the results revealed that the synthesized AuNPs had the desired properties, including uniform size, spherical shape, and negative surface charge, which were highly pertinent to biomolecular techniques.

3.2. Optimization of Nanozyme Activity Conditions. We examined the gold nanoparticles as a peroxidase catalyst and TMB as a substrate that might generate a blue color in H₂O₂. For colorimetric detection, the most desirable substrates quickly produce intensely colored reaction products. When the analyte amounts span a wide range of concentrations (large dynamic range), then it is more suitable to use substrates that produce color over a more extended period (15 to 30 min) because then, one can detect the broader range of analyte-

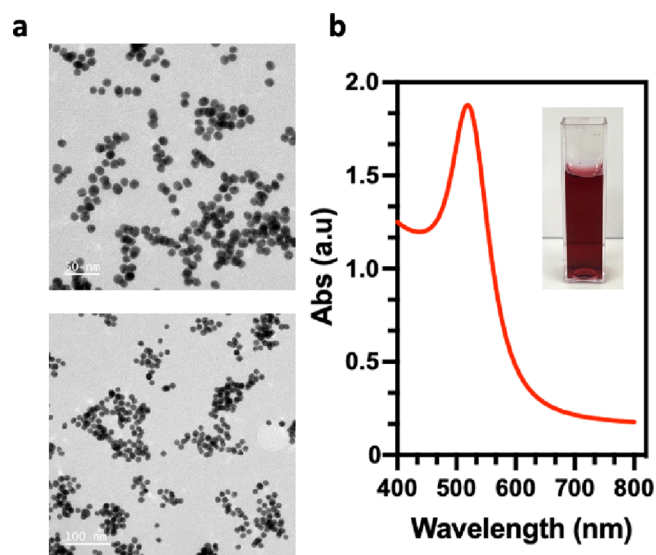


Figure 1. TEM images with scales of 50 and 100 nm (a) and UV-vis spectra in the wavelength range of 400 to 800 nm of AuNPs.

dependent color intensities.¹⁷ In this situation, the reaction period was chosen to be 30 min in all of our experiments. Figure 2a,c demonstrates that the nanozyme activity achieved

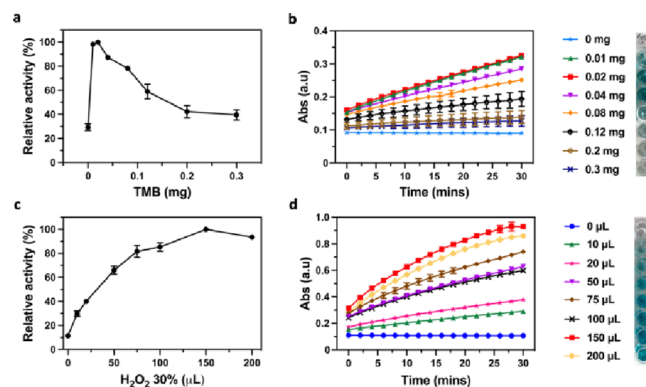


Figure 2. Effect of TMB (a, b) and H₂O₂ (c, d) concentration on nanozyme activity for 30 min (a, c) and within 30 min measured by signal absorption at 650 nm (b, d). The different concentrations of TMB and H₂O₂ were presented in panels (b) and (d), respectively.

the highest performance at 0.02 mg of TMB and 150 μL of H₂O₂, as the blue color was the strongest at those points after 30 min of incubation. The activities decreased as the TMB concentrations increased; however, the higher the volumes of H₂O₂ were, the greater the nanozyme signals that were measured. It could be explained that a continuous rise in TMB concentration might inhibit the activity of the nanozyme.

On the other hand, the nanozyme signals were elevated until the 30% H₂O₂ concentration reached 100 μL . The reactions continued in a reduction and oxidation cycle, which only occurred at a sufficient TMB amount in a particular concentration ratio of nanozyme and H₂O₂ (Figure 2a). The reaction signals of the kinetic study for the catalytic oxidation of TMB gradually rose as measured within 30 min (Figure 2b,d). As a result, 0.02 mg of TMB and 150 μL of 30% H₂O₂ were chosen for all experiments henceforth.

It has been reported that the AuNPs have possessed peroxidase-mimicking activity.^{18,19} Figure 3 reveals the real-

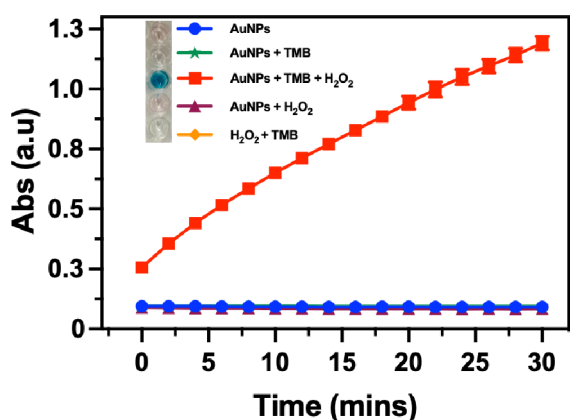


Figure 3. Evaluation of nanozyme activity in the presence of TMB and H_2O_2 measured by signal absorption at 650 nm. The experiments were conducted in five groups: only AuNPs, AuNPs + TMB, AuNPs + TMB + H_2O_2 , AuNPs + H_2O_2 , and H_2O_2 + TMB. Error bars represent the standard deviation of three repeated measurements.

time visual observation of the reaction in 30 min. The mixtures of AuNPs and TMB, AuNPs and H_2O_2 , and H_2O_2 and TMB were colorless, suggesting that AuNPs could not catalyze the oxidation of TMB when H_2O_2 was absent; therefore, the absorption at 650 nm was not observed. The data demonstrated that the formation of the blue color due to the TMB substrate oxidation only appeared under the coaction of nanozyme and H_2O_2 , which positively confirmed the activity of nanozyme as a catalyst.

3.3. Optimization of Staining Enhancement. Until now, several kinds of nanoparticles have been found to be peroxidase-like, modified to enhance the catalytic activities, including cysteamine-AuNPs,²⁰ chitosan-AuNPs,²¹ BSA-Au nanoclusters,²² $\text{Au}@\text{Fe}_3\text{O}_4$,²³ and $\text{Au}@\text{carbon dots}$.²⁴ The staining enhancement has improved color intensity for DNA membrane microarrays based on the seed-mediated growth of AuNP labels by HAuCl_4 and hydroxylamine.²⁵ Hydroxylammonium chloride was employed as the reductant in the staining process, capable of reducing Au^{3+} to form Au^0 , and the reduction could be catalyzed by the surface of AuNPs.²⁶ The concentrations of HAuCl_4 and $\text{NH}_2\text{OH}\cdot\text{HCl}$ would affect the growth of Au seeds, thus influencing colorimetric immunoreactions. In this work, we examined which concentrations of HAuCl_4 and $\text{NH}_2\text{OH}\cdot\text{HCl}$ were optimized for the staining enhancement procedure. The nanozyme activity was demonstrated to expose the highest signals at 2 mM HAuCl_4 (Figure 4a) and 10 mM $\text{NH}_2\text{OH}\cdot\text{HCl}$ (Figure 4b). With a higher concentration of HAuCl_4 , the solutions changed from pale pink to yellow (Figure 4a), whereas they were steadily stable as dark pink and finally changed to gray at 150 mM in the case of the $\text{NH}_2\text{OH}\cdot\text{HCl}$ concentrations (Figure 4b).

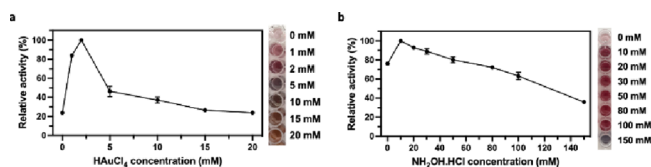


Figure 4. Effect of HAuCl_4 (a) and $\text{NH}_2\text{OH}\cdot\text{HCl}$ (b) concentrations on staining enhancement measured by signal absorption at 650 nm. The different molar concentrations of HAuCl_4 and $\text{NH}_2\text{OH}\cdot\text{HCl}$ were presented in panels (a) and (b), respectively.

We experimented with the concentrations of HAuCl_4 and $\text{NH}_2\text{OH}\cdot\text{HCl}$ in an optimized 1:5 ratio. Figure 5 reveals that

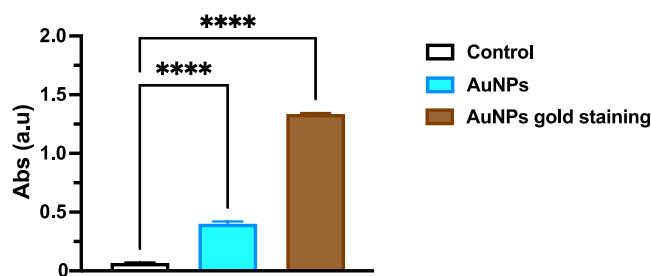


Figure 5. Evaluation of the nanozyme activity of bare AuNPs and AuNPs with staining enhancement measured by signal absorption at 650 nm. The experiments were conducted in control, AuNPs, and AuNPs staining. Error bars represented the standard deviation of three repeated measurements.

the AuNPs with staining enhancement activity were statistically approximately three times higher than the bare AuNPs. These results indicated that the nanozyme, after staining enhancement, possessed better action and that the employment of staining enhancement was feasible.

3.4. Optimization of Nano-ELISA Conditions. Different strategies for binding antibodies to AuNPs include direct coating, PEG-coated AuNPs with covalently bound antibodies,²⁷ and streptavidin-coated AuNPs with biotinylated antibodies.²⁷ Passive adsorption has been the traditional method for attaching proteins to nanoparticles and is still widely used by taking advantage of the intermolecular forces between molecules and surfaces. The antibody surface coverage was more excellent for direct adsorption than antibodies–nanoparticles covalent binding, indicating that significantly more antibodies were immobilized via nonspecific adsorption than covalent bonding.²⁸ Optimum conditions for *Kleb* Ab–AuNPs passive conjugation were obtained at pH 9 at RT, where no salt aggregation was obtained. This experiment also evaluated which concentration of the *K. pneumoniae* antibody was optimal for conjugation. When the *Kleb* Ab concentration increased, the nanozyme activity was inhibited, the strongest by nearly 35% at 15 μL of 1 μM *Kleb* Ab, which revealed no change in color after 30 min of incubation (Figure 6). Depending on the concentration of *Kleb* Ab, the activity of nanozyme remained stable in a range from 3 to 7 μL of 1 μM and then slightly decreased after 10 μL . It could confirm that

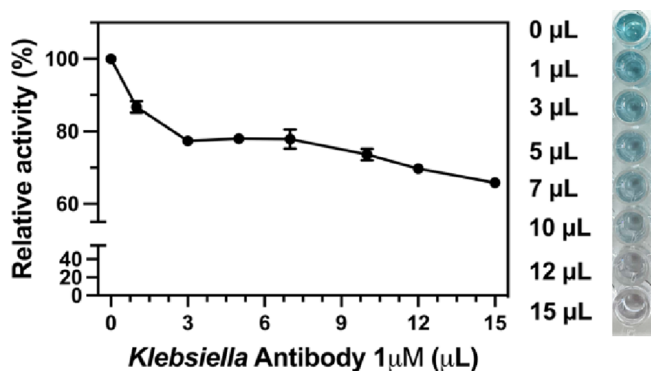


Figure 6. The effect of antibody concentration on nanozyme activity for 30 min was measured by signal absorption at 650 nm. The different molar concentrations of antibodies were presented.

the *Kleb* Abs were successfully conjugated on the nanoparticle's surface. However, surface modification, such as protein adsorption, slightly decreased the peroxidase-mimic activity of the nanozymes due to the active sites on the surface being shielded from interacting with substrates.¹⁶ Hence, we chose the concentration of *Kleb* Ab at 5 μ L of 1 μ M due to the sufficient amount of *Kleb* Ab in conjugation and nanozyme activity detected at the adsorption wavelength of 650 nm.

3.5. Determination of Cutoff, Limit of Detection (LoD), and Limit of Quantification (LoQ) of Nano-ELISA with Staining Enhancement. The OD of 0.099 at 650 nm was calculated as the cut-off value for the nano-ELISA (Figure S2). With the staining enhancement, the cut-off value was higher at 0.158 (Figure 7), determining that samples with OD

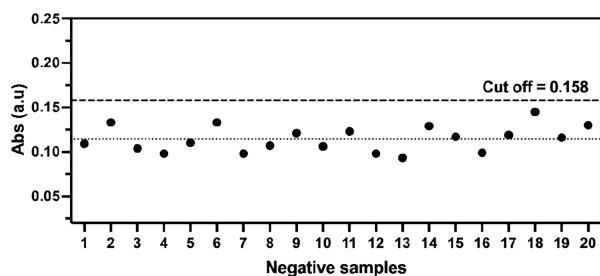


Figure 7. Determination of the cutoff value for nano-ELISA with staining enhancement. The mean value plus the standard deviation of 3 times was used as the cutoff value.

values higher than 0.158 are considered positive, and those with lower ODs were negative. The sensitivity and the linear response range of the nano-ELISA with staining enhancement were investigated by measuring the OD₆₅₀ for *K. pneumoniae* detection from 10¹ to 10⁸ CFUs/mL (Figure 8a). The linear

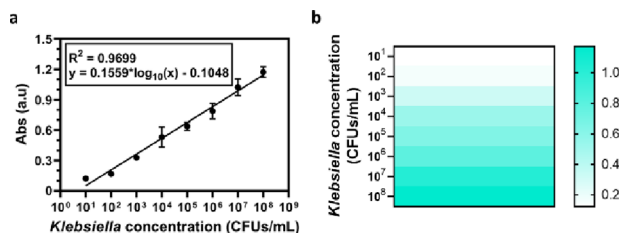


Figure 8. Calibration curve of *K. pneumoniae* with serial dilution concentrations from 10¹ to 10⁸ CFUs/mL. (a) Blue green-scale gradient heat map of *K. pneumoniae* detection range from 10¹ to 10⁸ CFUs/mL (b) in nano-ELISA with staining enhancement.

regression equation was determined to be $y = 0.1559 \log_{10}(x) - 0.1048$. The curve demonstrated a highly positive correlation between the *K. pneumoniae* concentration (CFUs/mL) and OD₆₅₀ signals ($R^2 = 0.9699$). The LoD and LoQ were calculated to be 36.230 and 78.857 CFUs/mL, respectively. Nano-ELISA with staining enhancement could detect as low as 1×10^2 CFUs/mL, which was 100 times higher than nano-ELISA with the bare AuNPs (Figure S3). The blue-green-scale gradient heat map showed that the color of the immuno-reactions changed from white to solid blue-green in direct proportion to the *K. pneumoniae* concentrations (Figure 8b).

3.6. Specificity Analysis of Nano-ELISA with Staining Enhancement. Apart from the sensitivity, specificity is the most crucial key affecting factor guaranteeing the feasibility of the AuNPs–*Kleb* Ab conjugation immunoassay. To investigate

the specificity of nano-ELISA for *K. pneumoniae* detection, we performed the immune reactions with other nontarget bacteria, including *P. aeruginosa*, *E. coli*, *C. perfringens*, *S. aureus*, and *S. typhimurium* (Figure 9). As can be seen clearly in Figure 9, *K.*

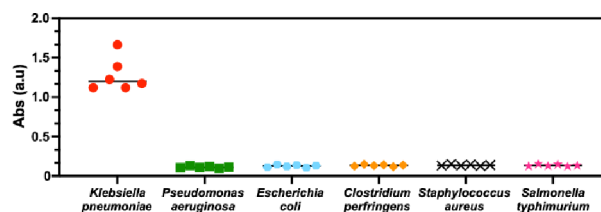


Figure 9. Specificity analysis of nano-ELISA for common pathogens, including *P. aeruginosa*, *E. coli*, *C. perfringens*, *S. aureus*, *S. typhimurium*, and *K. pneumoniae*.

pneumoniae positive sample (10⁸ CFUs/mL) signals were detected above 1 (a.u), indicating that the AuNPs–*Kleb* Ab conjugation attached to the *K. pneumoniae* bacteria during the incubation as the *Kleb* Ab conjugated with AuNPs specific to *K. pneumoniae*. In contrast, the other bacterial absorbance signals were below the cut-off value. These results demonstrated that our nano-ELISA procedure could be resistant to interference and could detect *K. pneumoniae* specifically.

K. pneumoniae has been detected by various kinds of techniques that can achieve high sensitivity and specificity. A MIP-based electrochemical biosensor was developed to measure the changes in electrical signals in different concentrations of *K. pneumoniae* ranging from 10 to 10⁵ CFU/mL, with a high linear response.²⁹ Detection of *Enterococcus faecalis* (G+), *K. pneumoniae* (G–), *P. aeruginosa* (G–), and *Candida tropicalis* was assessed in the same recognition range from 10¹ to 10⁵ CFUs/mL using mastoparan-capped magnetic nanoparticles for electrochemical detection.³⁰ Furthermore, a study reported a portable in-flow magnetic transduction-based instrument capable of rapid and highly sensitive detection of whole-bacterial cells in complex matrices, providing a Yes/No result with 100% sensitivity and 80.8% specificity for the detection of *K. pneumoniae* cells in laboratory samples.³¹ Compared to these methods, our results indicated that the novel nano-ELISA technique could detect *K. pneumoniae* with higher sensitivity, linearity, and specificity (Table 1).

4. CONCLUSIONS

In conclusion, a colorimetric, cost-effective, and less time-consuming immunoassay was successfully performed for *K. pneumoniae* detection. We optimized the experimental conditions of each component in the immunoreactions, including the TMB substrate, H₂O₂, HAuCl₄, and NH₂OH·HCl concentrations for staining enhancement. The catalytic nanozyme activity exhibited excellent catalytic efficiency, which was suppressed by nearly 35% after *K. pneumoniae* antibody conjugation. However, staining was enhanced three times compared to the bare AuNPs, capable of *K. pneumoniae* detection as low as 10² CFUs/mL, which was found to be sufficient for detecting *K. pneumoniae* in real-world applications. Our enhanced nano-ELISA was found to achieve a high linear response, with an R^2 value of 0.9699.

It was demonstrated that the nano-ELISA strategy has the advantages of high sensitivity, strong specificity, and excellent stability. As a proof of concept for appropriate biosensors with

Table 1. Comparison of the Proposed Method with the Other *K. pneumoniae* Detection Methods

| method | sensitivity | remark | ref |
|---|----------------------------|---|-----------|
| PCR-ELISA | 6.0 ng | 16S rDNA detected by anti-DIG–peroxidase conjugate | 32 |
| indirect ELISA | 2.99×10^7 CFUs/mL | high specificity but low sensitivity | 33 |
| IC-LAMP | 4 CFUs/mL | beads-mAb 1E6- <i>K. pneumoniae</i> used for LAMP assay | 34 |
| label-free multiple cross displacement amplification (MCDA) assay | 480 CFUs/mL | supplemented with AUDG enzyme to eliminate false-positive results | 4 |
| immunomagnetic assay | Yes/No result | low specificity but fast and convenient | 31 |
| molecularly imprinted polymer (MIP) | 10 CFUs/mL | high sensitivity but high standard error | 29 |
| nano-ELISA | 10^2 CFUs/mL | high specificity and sensitivity | this work |

nanozyme, nano-ELISA was augmented for *K. pneumoniae* detection using AuNPs–*K. pneumoniae* antibody conjugation and staining signal enhancement.

■ ASSOCIATED CONTENT

SI Supporting Information

The Supporting Information is available free of charge at <https://pubs.acs.org/doi/10.1021/acsomega.3c07503>.

Dynamic light scattering (DLS) measurements for the hydrodynamic diameter of the gold nanoparticles; zeta potential of the gold nanoparticles; determination of the cutoff value for nano-ELISA; calibration curve of *K. pneumoniae* with serial dilution concentrations from 10^1 to 10^8 CFUs/mL (PDF)

■ AUTHOR INFORMATION

Corresponding Author

Lien Truong T N – Vietnam-Korea Institute of Science and Technology, Hanoi 100000, Vietnam; Email: truongtlien@gmail.com

Authors

Thu Thao Pham – Graduate University of Science and Technology, Vietnam Academy of Science and Technology, Hanoi 100000, Vietnam; Vietnam-Korea Institute of Science and Technology, Hanoi 100000, Vietnam; orcid.org/0000-0001-7763-6486

Thien-Kim Le – Vietnam-Korea Institute of Science and Technology, Hanoi 100000, Vietnam; orcid.org/0000-0001-5239-4943

Nguyen T. T. Huyen – Vietnam-Korea Institute of Science and Technology, Hanoi 100000, Vietnam

Nam Luyen Van – Vietnam-Korea Institute of Science and Technology, Hanoi 100000, Vietnam

Tin Phan Nguy – Vietnam-Korea Institute of Science and Technology, Hanoi 100000, Vietnam; School of Engineering Physics, Hanoi University of Science and Technology, Hanoi 100000, Vietnam; orcid.org/0000-0002-3294-9822

Dai Lam Tran – Institute of Tropical Technology, Vietnam Academy of Science and Technology, Hanoi 100000, Vietnam

Complete contact information is available at:

<https://pubs.acs.org/doi/10.1021/acsomega.3c07503>

Notes

The authors declare no competing financial interest.

■ ACKNOWLEDGMENTS

All authors are grateful for the financial support from Vingroup Innovation Foundation (grant no. VINIF.2022.DA00032).

■ REFERENCES

- (1) Effah, C. Y.; Sun, T.; Liu, S.; Wu, Y. *Klebsiella pneumoniae*: an increasing threat to public health. *Ann. Clin. Microbiol. Antimicrob.* **2020**, *19* (1), 1–9.
- (2) Gera, K.; Roshan, R.; Varma-Basil, M.; Shah, A. Chronic pneumonia due to *Klebsiella oxytoca* mimicking pulmonary tuberculosis. *Adv. Respir. Med.* **2015**, *83* (5), 383–386.
- (3) Russo, T. A.; Marr, C. M. Hypervirulent *klebsiella pneumoniae*. *Clin. Microbiol. Rev.* **2019**, *32* (3), No. e00001.
- (4) Wang, Y.; Yan, W.; Wang, Y.; Xu, J.; Ye, C. Rapid, sensitive and reliable detection of *Klebsiella pneumoniae* by label-free multiple cross displacement amplification coupled with nanoparticles-based biosensor. *J. Microbiol. Methods* **2018**, *149*, 80–88.
- (5) Donelli, G.; Vuotto, C.; Mastromarino, P. Phenotyping and genotyping are both essential to identify and classify a probiotic microorganism. *Microb. Ecol. Health Disease* **2013**, *24* (1), 20105.
- (6) Das, B.; Franco, J. L.; Logan, N.; Balasubramanian, P.; Kim, M. I.; Cao, C. Nanozymes in point-of-care diagnosis: an emerging futuristic approach for biosensing. *Nano-Micro Lett.* **2021**, *13*, 1–51.
- (7) Deng, H.-H.; Hong, G.-L.; Lin, F.-L.; Liu, A.-L.; Xia, X.-H.; Chen, W. Colorimetric detection of urea, urease, and urease inhibitor based on the peroxidase-like activity of gold nanoparticles. *Anal. Chim. Acta* **2016**, *915*, 74–80.
- (8) Das, B.; et al. Peroxidase-Mimicking Activity of Biogenic Gold Nanoparticles Produced from *Prunus nepalensis* Fruit Extract: Characterizations and Application for the Detection of *Mycobacterium bovis*. *ACS Appl. Bio Mater.* **2022**, *5* (6), 2712–2725.
- (9) Guo, C.; Liu, D.; Xu, W.; He, L.; Liu, S. Accelerating the peroxidase-and glucose oxidase-like activity of Au nanoparticles by seeded growth strategy and their applications for colorimetric detection of dopamine and glucose. *Colloids Surf. A Physicochem Eng. Asp* **2023**, *658*, No. 130555.
- (10) Yao, S.; Li, J.; Pang, B.; Wang, X.; Shi, Y.; Song, X.; Xu, K.; Wang, J.; Zhao, C.; et al. Colorimetric immunoassay for rapid detection of *Staphylococcus aureus* based on etching-enhanced peroxidase-like catalytic activity of gold nanoparticles. *Microchim. Acta* **2020**, *187*, 1–8.
- (11) Turkevich, J.; Stevenson, P. C.; Hillier, J. A study of the nucleation and growth processes in the synthesis of colloidal gold. *Discuss. Faraday Soc.* **1951**, *11*, 55–75.
- (12) Abbott, M.; et al. Validation procedures for quantitative food allergen ELISA methods: community guidance and best practices. *J. AOAC Int.* **2010**, *93* (2), 442–450.
- (13) Yeh, Y.-C.; Creran, B.; Rotello, V. M. Gold nanoparticles: preparation, properties, and applications in bionanotechnology. *Nanoscale* **2012**, *4* (6), 1871–1880.
- (14) Yazdani, S.; et al. Model for gold nanoparticle synthesis: Effect of pH and reaction time. *ACS Omega* **2021**, *6* (26), 16847.
- (15) Lou, D.; et al. Peroxidase-like activity of gold nanoparticles and their gold staining enhanced ELISA application. *J. Nanosci. Nanotechnol* **2018**, *18* (2), 951–958.
- (16) Liu, B.; Liu, J. Surface modification of nanozymes. *Nano Res.* **2017**, *10*, 1125–1148.
- (17) Minic, R.; Zivkovic, I., "Optimization, Validation and Standardization of ELISA," in *Norovirus*, G., Mózsi, Ed., Rijeka: IntechOpen, 2020; p. Ch. 2. doi: DOI: 10.5772/intechopen.94338.

- (18) Liu, Y.; Wang, C.; Cai, N.; Long, S.; Yu, F. Negatively charged gold nanoparticles as an intrinsic peroxidase mimic and their applications in the oxidation of dopamine. *J. Mater. Sci.* **2014**, *49*, 7143–7150.
- (19) Li, R. S.; Liu, H.; Chen, B. B.; Zhang, H. Z.; Huang, C. Z.; Wang, J. Stable gold nanoparticles as a novel peroxidase mimic for colorimetric detection of cysteine. *Anal. Methods* **2016**, *8* (11), 2494–2501.
- (20) Zhao, D.; Chen, C.; Lu, L.; Yang, F.; Yang, X. A label-free colorimetric sensor for sulfate based on the inhibition of peroxidase-like activity of cysteamine-modified gold nanoparticles. *Sens Actuators B Chem.* **2015**, *215*, 437–444.
- (21) Jiang, C.; Zhu, J.; Li, Z.; Luo, J.; Wang, J.; Sun, Y. Chitosan–gold nanoparticles as peroxidase mimic and their application in glucose detection in serum. *RSC Adv.* **2017**, *7* (70), 44463–44469.
- (22) Chang, Y.; Zhang, Z.; Hao, J.; Yang, W.; Tang, J. BSA-stabilized Au clusters as peroxidase mimetic for colorimetric detection of Ag⁺. *Sens Actuators B Chem.* **2016**, *232*, 692–697.
- (23) Zhang, S.; et al. A strongly coupled Au/Fe₃O₄/GO hybrid material with enhanced nanozyme activity for highly sensitive colorimetric detection, and rapid and efficient removal of Hg²⁺ in aqueous solutions. *Nanoscale* **2015**, *7* (18), 8495–8502.
- (24) Zheng, C.; Ke, W.; Yin, T.; An, X. Intrinsic peroxidase-like activity and the catalytic mechanism of gold@ carbon dots nanocomposites. *RSC Adv.* **2016**, *6* (42), 35280–35286.
- (25) Presnova, G. V.; Zhdanov, G. A.; Filatova, L. Y.; Ulyashova, M. M.; Presnov, D. E.; Rubtsova, M. Y. Improvement of Seed-Mediated Growth of Gold Nanoparticle Labels for DNA Membrane-Based Assays. *Biosensors (Basel)* **2023**, *13* (1), 2.
- (26) Brown, K. R.; Natan, M. J. Hydroxylamine seeding of colloidal Au nanoparticles in solution and on surfaces. *Langmuir* **1998**, *14* (4), 726–728.
- (27) Conrad, M.; Proll, G.; Builes-Münden, E.; Dietzel, A.; Wagner, S.; Gauglitz, G. Tools to compare antibody gold nanoparticle conjugates for a small molecule immunoassay. *Microchim. Acta* **2023**, *190* (2), 62.
- (28) Tripathi, K.; Driskell, J. D. Quantifying bound and active antibodies conjugated to gold nanoparticles: A comprehensive and robust approach to evaluate immobilization chemistry. *ACS Omega* **2018**, *3* (7), 8253–8259.
- (29) Pintavirooj, C.; Vongmanee, N.; Sukjee, W.; Sangma, C.; Visitsattapongse, S. Biosensors for *Klebsiella pneumoniae* with molecularly imprinted polymer (MIP) technique. *Sensors* **2022**, *22* (12), 4638.
- (30) da Silva Junior, A. G.; Frias, I. A. M.; Lima-Neto, R. G.; Franco, O. L.; Oliveira, M. D. L.; Andrade, C. A. S. Electrochemical detection of gram-negative bacteria through mastoparan-capped magnetic nanoparticle. *Enzyme Microb Technol.* **2022**, *160*, No. 110088.
- (31) Soares, A. R.; et al. On-site magnetic screening tool for rapid detection of hospital bacterial infections: Clinical study with *Klebsiella pneumoniae* cells. *Biosens Bioelectron X* **2022**, *11*, No. 100149.
- (32) Tayebbeh, F.; Amani, J.; Nazarian, S.; Moradyar, M.; Mirhosseini, S. A. Molecular diagnosis of clinically isolated *Klebsiella pneumoniae* strains by PCR-ELISA. *J. Appl. Biotechnol. Rep.* **2016**, *3* (4), 501–505.
- (33) Chen, R.; Shang, H.; Niu, X.; Huang, J.; Miao, Y.; Sha, Z.; Qin, L.; Huang, H.; Peng, D.; Zhu, R.; et al. Establishment and evaluation of an indirect ELISA for detection of antibodies to goat *Klebsiella pneumoniae*. *BMC Vet. Res.* **2021**, *17*, 1–10.
- (34) Zhang, L.; et al. "Visual and rapid detection of *Klebsiella pneumoniae* by magnetic immunocapture-loop-mediated isothermal amplification assay,". *Jundishapur J. Microbiol* **2019**, *12*, No. e90016, DOI: 10.5812/jjm.90016.